Measurement Report: Abundance and fractional solubilities of aerosol metals in urban Hong Kong: Insights into factors that control aerosol metal dissolution in an urban site in South China

Junwei Yang,[1] Lan Ma,[1] Xiao He,[2] Wing Chi Au,[1] Yanhao Miao,[1] Wen-Xiong Wang,[1,3] Theodora Nah[1,3]*

[1]*School of Energy and Environment, City University of Hong Kong, Hong Kong SAR, China*

[2]*College of Chemistry and Environmental Engineering, Shenzhen University, Shenzhen 518060, China*

[3]*State Key Laboratory of Marine Pollution, City University of Hong Kong, Hong Kong SAR, China*

** To whom correspondence should be addressed: Theodora Nah (Email: theodora.nah@cityu.edu.hk)*

Abstract

Water-soluble metals are known to produce greater adverse human health outcomes than their water-insoluble forms. Although the concentrations of water-soluble aerosol metals are usually limited by atmospheric processes that convert water-insoluble metals to water-soluble forms, factors that control the solubilities of aerosol metals in different environments remain poorly understood. In this study, we investigated the abundance and fractional solubilities of different metals in size-fractionated aerosols collected at an urban site in Hong Kong, and identified the factors that modulated metal solubilities in fine aerosols. The concentrations of total and water-soluble metals in fine and coarse aerosols were the highest during the winter and spring seasons due to the long-range transport of air masses by northly prevailing winds from emission sources located in continental areas north of Hong Kong. The study-averaged metal fractional solubilities spanned a wide range for both fine (7.8 % to 71.2 %) and coarse (0.4 % to 47.9 %) aerosols, but higher fractional solubilities were typically observed for fine aerosols. Sulfate was found to be strongly associated with both the concentrations of water-soluble Cr, Fe, Co, Cu, Pb, and Mn and their fractional solubilities in fine aerosols, which implied that sulfate-driven acid processing likely played an important role in the dissolution of the water-insoluble forms for these six metals. Further analyses revealed that these strong associations were due to sulfate providing both the acidic environment and liquid water reaction medium needed for the acid dissolution process. Thus, the variability in the concentrations of water-soluble Cr, Fe, Co, Cu, Pb, and Mn and their fractional solubilities were driven by both the aerosol acidity levels and liquid water concentrations, which in turn were controlled by sulfate. These results highlight the roles that sulfate plays in the acid dissolution of metals in fine aerosols in Hong Kong. Our findings will likely also apply to other urban areas in South China, where sulfate is the dominant acidic and hygroscopic component in fine aerosols.

1. Introduction

Chronic exposures to atmospheric aerosols, especially those in the fine mode ($PM_{2.5}$, aerosols with aerodynamic diameter ≤ 2.5 μm), have been linked to a myriad of deleterious effects on human health, including morbidity and excessive deaths through respiratory and cardiovascular diseases (Brook et al., 2010; Cohen et al., 2017). Some of the aerosol chemical species cause majority of the adverse human health outcomes even though they comprise a small fraction of the overall aerosol mass (Phalen, 2004; Lippmann, 2014). Metals are ubiquitous chemical species that contribute significantly to airborne aerosol toxicity even though they are typically present in aerosols in trace quantities (Costa and Dreher, 1997a; Frampton et al., 1999; Ye et al., 2018; Zhao et al., 2021). Natural sources, especially mineral dust and sea spray, dominate the global sources of aerosol metals (Nriagu, 1989; Garrett, 2000; Deguillaume et al., 2005; Mahowald et al., 2018). However, anthropogenic sources such as industrial activities and vehicular traffic contribute substantial quantities of aerosol metals in urban environments (Garg et al., 2000; Adachi and Tainosho, 2004; Deguillaume et al., 2005; Lough et al., 2005; Birmili et al., 2006; Lee et al., 2007; Cheng et al., 2009; Li et al., 2013; Jiang et al., 2015; Mahowald et al., 2018).

Metals exist in aerosols in water-insoluble and water-soluble forms. Compared to their water-insoluble forms, water-soluble metals have higher bioavailability, which reportedly allows them to produce adverse human health outcomes (Costa and Dreher, 1997b; Heal et al., 2009; Fang et al., 2015; Gao et al., 2020a; He et al., 2021). Some water-soluble transition metal ions (e.g., Fe(II), Fe(III), Cu(I), Cu(II)) are redox-active species and serve as catalysts in reaction cycles (e.g., Fenton-like reactions) to enhance the *in vivo* production of reactive oxygen species (ROS) (e.g., ·OH, HO_2·, H_2O_2), which subsequently induce the physiological oxidative stress and inflammation involved in a variety of chronic and acute diseases (Bresgen and Eckl, 2015; Lakey et al., 2016; Bates et al., 2019). A recent epidemiologic study reported that water-soluble Fe concentrations in $PM_{2.5}$ showed strong correlations with cardiovascular-related emergency department visits in Atlanta (Ye et al., 2018). Less abundant water-soluble aerosol metals such as Cr and Pb are also known to exhibit both carcinogenic and noncarcinogenic risks to adults and children despite their small quantities (He et al., 2021).

Water-soluble metals also play important roles in ocean biogeochemistry and atmospheric processes. Atmospheric aerosol deposition is an important source of bioavailable dissolved metals in open oceans. The dissolved metals serve as nutrients, and in some cases toxins, for various aquatic species (De Baar et al., 2005; Boyd et al., 2007; Paytan et al., 2009; Jordi et al., 2012). Some transition metal ions such as Fe(III) and Mn(II) ions can facilitate the formation and aging of organic aerosols (Chu et al., 2013; Al-Abadleh, 2015; Slikboer et al., 2015; Chu et al., 2017; Al-Abadleh, 2021), The coupled redox cycling of Cu(I)/Cu(II) and Fe(II)/Fe(III) ions in aerosols has been proposed to be an important mechanism for the uptake of gas-phase HO_2 in aqueous aerosols, which has important implications for the tropospheric OH radical and O_3 budget (Mao et al., 2013; Mao et al., 2017). Mn(II)-catalyzed oxidation of SO_2 on aqueous aerosol surfaces reportedly contributes more than 90 % of the sulfate production during wintertime haze events in China (Wang et al., 2021).

Aerosol metals are primarily emitted into the atmosphere in water-insoluble forms (Nriagu, 1989). While water-soluble aerosol metals can be emitted directly into the atmosphere (Fang et al., 2015), the concentrations of water-soluble aerosol metals are likely limited by atmospheric processes that convert the water-insoluble metal forms to water-soluble forms (Mahowald et al., 2018). Given the important roles that water-soluble aerosol metals play in adverse human health outcomes and atmospheric processes, it is necessary to understand the factors that modulate the atmospheric processing, and hence the solubility, of aerosol metals. Aerosol Fe dissolution has been the focus of most previous studies. A wide range (<1 % to 98 %) of fractional solubilities (ratio of the water-soluble metal mass concentration to the total metal mass concentration) has been reported for Fe in atmospheric aerosols (Mahowald et al., 2018). Anthropogenic-influenced aerosols generally have higher Fe solubility than fresh mineral dust (Sedwick et al., 2007; Schroth et al., 2009; Oakes et al., 2012). However, Fe solubility varies substantially in aerosols in different urban environments with high levels of anthropogenic activities (e.g., 1 % to 12 % in four cities in East China (Zhu et al., 2020) vs. around 20 % to 50 % in Hong Kong, South China (Jiang et al., 2014; Jiang et al., 2015). Although there are a number of atmospheric processes that can influence aerosol metal solubilities, acid processing and the formation of stable Fe-organic complexes are two key

chemical processes known to enhance aerosol Fe dissolution (Deguillaume et al., 2005; Ingall et al., 2018; Tao and Murphy, 2019; Giorio et al., 2022). At present, it remains difficult to explain the variability of aerosol Fe solubility in urban environments since the extent to which aerosol Fe dissolution is controlled by factors such as aerosol acidity and/or the presence of organic ligands (e.g., oxalate) in different urban environments is still not well understood. Even less is known about the factors that control the solubilities of other aerosol metals beyond Fe.

Hong Kong is a highly developed, densely populated city in the Guangdong-Hong Kong-Macau Great Bay Area (GBA) urban agglomeration, which is a large business and economic hub located in the southern part of China. While there have been some studies on the fractional solubilities of various aerosol metals in Hong Kong (Jiang et al., 2014; Jiang et al., 2015), to the best of our knowledge, there has not been a study that has investigated the factors that control the solubilities of aerosol metals in Hong Kong. In this study, we investigated the abundance and fractional solubilities of ten metals (Fe, Cu, Al, V, Cr, Mn, Co, Ni, Cd, and Pb) in aerosols at an urban site in Hong Kong. Our main goal is to identify the key factors that control the solubilities of metals in fine aerosols since they are believed to exert higher toxicity than coarse aerosols due to their small sizes. We focus primarily on aerosol metal dissolution through the acid processing and/or metal-organic complexation mechanisms. Hence, other aerosol species were also measured for comparisons to total and water-soluble metals. The measured aerosol inorganic ion composition was used as inputs for a thermodynamic model to determine the aerosol acidity levels, liquid water concentrations, and pH.

2. Methods

2.1. Ambient sampling

The sampling campaign took place at ground level next to a road in Kowloon Tong (22.3367° N, 114.1724° E). Kowloon Tong is located in the southern side of Hong Kong, and it is primarily a residential and commercial district which is close to Mongkok, one of the busiest commercial and most densely populated areas in Hong Kong with high density traffic flow. Weekly size-fractionated aerosol samples were collected on 7 March 2021 to 4 April 2021 (spring season), 23 to 30 June 2021 and 7 to 14 July 2021 (summer season), 13 September

2021 to 11 October 2021 (fall season), and 15 December 2021 to 26 January 2022 (winter season). Back-trajectories calculations calculated by the Hybrid Split-Particle Lagrangian Integrated Trajectory (HYSPLIT) model using meteorological data from NCEP/NCAR Reanalysis (2.5° latitude-longitude grid) showed that the sampling site was under the influence of continental and marine air masses during the sampling periods, though the contributions of these air masses varied with the season (Figure S1).

An eleven stage Micro-Orifice Uniform Deposit Impactor (MOUDI) (Model 110, MSP Corp., USA) was used to collect and divide aerosols into different aerosol size bins under ambient conditions. Aerosols were collected on prebaked 47 mm diameter quartz filters (Tissuquartz 2500QAT-UP, Pall Corp., USA). The nominal cut points for the MOUDI eleven impactor stages were 0.056 μm, 0.1 μm, 0.18 μm, 0.32 μm, 0.56 μm, 1.0 μm, 1.8 μm, 3.2 μm, 5.6 μm, 10 μm, and 18 μm. In the discussion below, for simplicity, we refer to aerosols collected on impactor stages with nominal cut points 0.056 μm, 0.1 μm, 0.18 μm, 0.32 μm, 0.56 μm, 1.0 μm, and 1.8 μm as "fine aerosols", while aerosols collected on impactor stages with nominal cut points 3.2 μm, 5.6 μm, 10 μm, and 18 μm were referred to as "coarse aerosols". Aerosols were collected continuously for seven days (i.e., 24 hours × 7 days). This resulted in a total of four, two, four, and six weekly sets of aerosol filter samples collected during the spring, summer, fall, and winter seasons, respectively. After collection, the aerosol filter samples were immediately extracted for chemical analysis.

Thermodynamic model calculations used to determine the aerosol acidity levels, liquid water concentrations, and pH (Section 2.3) require gas-phase NH_3 concentrations, ambient temperature and relative humidity (RH) as model inputs. Hence, weekly NH_3 measurements were performed during each sampling period using four passive sampling devices (PSDs) and pre-coated collection pads (PS-100 and PS-154, Ogawa & Co., Pompano Beach, FL), except from 7 to 28 March 2021. The exposed PSD collection pads were extracted in purified deionized water (18.2 MΩ-cm) using the protocol recommended by the manufacturer. These aqueous extracts were subsequently analyzed by ion chromatography (Section 2.2) to determine the average NH_3 concentration during the sampling period. A Vantage Vue Weather Station (Model 6250, Davis Instruments, USA) was used to measure ambient temperature and

RH during each sampling period.

2.2. Chemical analysis

Each aerosol filter sample was cut into four equal pieces for chemical analysis of different chemical components. One of the four pieces was extracted in purified deionized water via sonication (1 hour), followed by high speed vortexing at 3000 rpm (15 minutes). The resulting aqueous extract was filtered using 0.22 μm pore size nylon filters (Jinteng Instrument Co., Tianjin, China) before it was analyzed by a Total Organic Carbon (TOC) analyzer (TOC-VCSH, Shimadzu, Japan) to determine the concentration of water-soluble organic carbon (WSOC). The TOC analyzer has a limit of detection (LOD) of 0.5 mg L^{-1}. The second filter piece was similarly extracted in purified deionized water via sonication (1 hour) and high speed vortexing at 3000 rpm (15 minutes), and filtered using 0.22 μm pore size nylon filters before it was analyzed by an ion chromatography (IC) system (Dionex ICS-1100, ThermoFisher Scientific, USA) using an isocratic method to determine the concentrations of water-soluble anions (NO_3^-, SO_4^{2-}, Cl^-, and $C_2O_4^{2-}$) and cations (NH_4^+, Na^+, K^+, Ca^{2+}, and Mg^{2+}). Anion separation was achieved using a 4 × 250 mm anion exchange column (Dionex IonPac AS18, ThermoFisher Scientific, USA) equipped with a 4 × 50 mm guard column (Dionex IonPac AG18, ThermoFisher Scientific, USA). Cation separation was achieved using a 4 × 250 mm cation exchange column (Dionex IonPac CS12A, ThermoFisher Scientific, USA) equipped with a 4 × 50 mm guard column (Dionex IonPac CG12A, ThermoFisher Scientific, USA). 16 mM potassium hydroxide and 31 mM methanesulfonic acid were used as eluents at a flowrate of 1.0 mL min^{-1} for the anion and cation separations, respectively. The cation IC method was also used to analyze the aqueous extracts from the exposed PSD collection pads to determine the average NH_3 concentration during each sampling week. The LODs for the cation IC method were 0.025 mg L^{-1} for NH_4^+, Na^+, and Mg^{2+}, and 0.025 mg L^{-1} for K^+ and Ca^{2+}. The LODs for the anion IC method were 0.125 mg L^{-1} for NO_3^-, SO_4^{2-}, and $C_2O_4^{2-}$, and 0.025 mg L^{-1} for Cl^-.

The remaining two filter pieces were used for metal analysis. One filter piece was extracted with purified deionized water in metal-free centrifuge tubes via sonication (1 hour), followed by high speed vortexing at 3000 rpm (15 minutes). The resulting aqueous extract was

filtered using 0.22 μm pore size nylon filters, and acidified with 2 % HNO_3 prior to storage at 4 °C before chemical analysis of water-soluble metals. The filterable metal fraction in the water extracts, defined in this study as water-soluble metals, will include all dissolved metal forms and any colloidal particles with diameters smaller than 0.22 μm. This assumes that all colloidal particles with diameters smaller than 0.22 μm can penetrate through the syringe filter, and that the syringe filter's retention efficiency of particles with diameters larger than 0.22 μm is 100 %. The exact sizes and distribution of metal colloidal particles in the filterable metal fraction in water extracts in this study are not known. However, Yang et al. (2021) recently reported that around 84% of Fe and Cu colloidal particles that penetrated through 0.45 μm syringe filters had nominal diameters smaller than 4 nm. The remaining 16% of Fe and Cu colloidal particles had nominal diameters between 4 nm and 0.45 μm, and they may be in water-insoluble forms (e.g., Fe and Cu oxides) so they may not be "true" water-soluble species. Hence, analogous to observations made by Yang et al (2021), it is possible that the filterable metal fractions in water extracts in this study contain some metals in water-insoluble forms with diameters smaller than 0.22 μm that penetrated through the 0.22 μm pore size filters. The last filter piece was extracted via acid digestion for chemical analysis of total metals. The acid digestion protocol we employed was adapted from published protocols (Jiang et al., 2014; Jiang et al., 2015). The filter piece was extracted in an acid digestion matrix (16 N HNO_3 and 12 N HCl at a 3:1 volume ratio) placed in a glass microwave vial using a microwave synthesizer (Initiator+, Biotage, Sweden). The microwave synthesizer's digestion temperature was ramped up to 150 °C, and then held for 15 min. This was followed by cooling and ventilation for 30 minutes. An evaporation and recovery treatment was next performed to remove Cl^- from the matrix to reduce its interference during chemical analysis. The digestion solution was heated to 200 °C on a hotplate. Once the solution was observed to be almost dry, 16 N HNO_3 was added to the solution. When the solution was observed to be almost dry the second time, 2 % HNO_3 was added to the solution. The resulting solution was filtered using 0.22 μm pore size nylon filters, and then stored at 4 °C before chemical analysis of total metals. A standard reference material of San Joaquin soil (SRM 2709a, NIST) was digested and analyzed using the same protocols to evaluate the metal recoveries. Recoveries of 59.4 % for Cr, 67.0 % for Al, 93.7 % for Fe,

93.6 % for Ni, 100.2 % for Co, 98.6 % for Pb, 95.8 % for Cu, 99.6 % for Mn, 70.5 % for V, and 94.3 % for Cd were observed.

The concentrations of ten water-soluble and total metals (^{27}Al, ^{51}V, ^{52}Cr, ^{55}Mn, ^{57}Fe, ^{59}Co, ^{60}Ni, ^{65}Cu, ^{111}Cd, and ^{208}Pb) were determined by an Inductively Coupled Plasma–Mass Spectrometry (ICP–MS) instrument (NexION 1000, PerkinElmer Inc., USA). The following parameters were used for the ICP-MS instrument: 0.98 L min^{-1} nebulizer gas flow, 1.2 L min^{-1} auxiliary gas flow, 15 L min^{-1} plasma gas flow, 5 mL min^{-1} He gas flow, 1600 W RF power, 35 rpm nebulizer pump rate, and 35 rpm sample pump rate. A multi-elemental calibration standard (IV-STOCK-13, Inorganic Ventures, USA) was used to quantify the ten water-soluble and total metals. An internal standard solution of ^{115}In (10 μg L^{-1}) was added to all samples and standards to monitor analytical drift. The LODs for ^{27}Al, ^{51}V, ^{52}Cr, ^{55}Mn, ^{57}Fe, ^{59}Co, ^{60}Ni, ^{65}Cu, ^{111}Cd, and ^{208}Pb were 87, 0.8, 2.8, 1.6, 277, 0.7, 4.6, 6.7, 1, and 0.4 ng L^{-1}, respectively. To identify the major sources of the aerosol metals, source apportionment was performed with positive matrix factorization (PMF) (Paatero and Tapper, 1994; Paatero, 1997) using the aerosol chemical components measured by the ICP-MS and IC. Details of the PMF method used can be found in Section S1 (SI).

2.3. Thermodynamic modeling

The thermodynamic model ISORROPIA-II was used to determine aerosol acidity levels, liquid water concentrations, and pH (Fountoukis and Nenes, 2007). Similar to the methodology employed by Fang et al. (2017), we ran ISORROPIA-II for each of the MOUDI impactor stages that collected fine aerosols. The measured water-soluble NH_4^+, SO_4^{2-}, NO_3^-, Cl^-, Na^+, Ca^{2+}, K^+, and Mg^{2+} ions for the aerosols collected on the MOUDI impactor stage, gas-phase NH_3, ambient temperature and RH were used as model inputs. Since gas-phase NH_3 measurements were not available from 7 to 28 March 2021, we used NH_3 measurements from 28 March to 4 April 2021 as model inputs for the spring calculations. The measured NH_3 concentrations during the study ranged from 3.60 μg m^{-3} to 8.18 μg m^{-3}, with a study-averaged concentration of 5.01 ± 1.25 μg m^{-3}. ISORROPIA-II was run in "forward" mode and under the assumption that the aerosols existed in a "metastable" equilibrium state (i.e., the aerosols only existed in

liquid form). These calculations assumed that the aerosols were in thermodynamic equilibrium with the gas phase. While fine aerosols satisfy this equilibrium condition, equilibrium between the gas and aerosol phases of coarse aerosols cannot be achieved due to kinetic limitations (Fountoukis et al., 2009). Thus, aerosol pH values were not calculated for coarse aerosols.

Fine aerosol pH values were calculated based on the molal definition (Pye et al., 2020):

$$pH = -\log_{10}\gamma_{H^+}H^+_{aq} = -\log_{10}\frac{1000H^+_{air}}{W_i+W_o} \cong -\log_{10}\frac{1000H^+_{air}}{W_i} \quad (1)$$

where γ_{H^+} is the hydronium ion activity coefficient, H^+_{aq} is the hydronium ion concentration within the ambient aerosol liquid water (mol L^{-1}), H^+_{air} is the hydronium ion concentration per volume of air (μg m^{-3}), and W_i and W_o are the aerosol liquid water concentrations (μg m^{-3}) associated with inorganic and organic species, respectively. H^+_{air} and W_i are the outputs provided by the ISORROPIA-II model, which assumes that γ_{H^+} is equals to unity. W_o can be estimated from the WSOC measurements using the approach described in Section S2 (SI). WSOC concentrations in the size-fractionated aerosols ranged from 0 to 4.6 μg m^{-3}. The inclusion of W_o into calculations did not impact aerosol pH significantly (Figure S2). Thus, only aerosol pH values calculated using W_i will be reported here. Similar to Fang et al. (2017), lower pH values were typically calculated for aerosols collected on MOUDI impactor stages with smaller nominal cut points (i.e., these aerosols had smaller aerodynamic aerosol diameters) due to the higher mass concentrations of sulfate in these smaller aerosols. The fine aerosols were mostly acidic, with about 74 % of the calculated pH values lying between 2 and 4.

3. Results and discussion

3.1. Total metals

Figure 1 shows the seasonal average mass concentrations of the ten measured total metals in size-fractionated aerosols. The size distributions of five of the metals (Al, Fe, Mn, V, and Cd) consistently exhibited a single mode. The modes for Mn, V, and Cd were predominantly found in the fine mode, while the modes for Fe and Al were predominantly found in the coarse aerosol mode. Figure 2a shows the seasonal average concentrations of the ten measured total metals in fine and coarse aerosols. For most of the metals, higher mass

concentrations were measured during the winter and/or spring seasons. This could be attributed to the long-range transport of polluted air masses by northly prevailing winds from emission sources located in continental areas north of Hong Kong (Figure S1). The metals could be arranged in the following order based on their abundances: Fe > Al > Cu > Co > Mn > Pb > Cr > Ni > V > Cd. This order of abundance was the same for both fine and coarse aerosols.

The mass concentrations of the two most abundant metals, Fe and Al, were usually higher than 10 ng m^{-3} in both fine and coarse aerosols. Fe, Al, and Cu had substantially higher mass concentrations in coarse aerosols than in fine aerosols. The positive correlations between the mass concentrations of Al with the mass concentrations of Fe and Cu were the strongest among the nine metals (R = 0.62 and R = 0.52, respectively) and statistically significant (Figure S3), which could be explained by large mass concentrations of Al, Fe, and Cu originating from similar sources. These three metals are known to originate mainly from dust sources (e.g., mineral dust and road dust) (Hopke et al., 1980; Garg et al., 2000; Adachi and Tainosho, 2004; Lough et al., 2005; Chow et al., 2022). This is consistent with results from our PMF source apportionment analysis, which showed that the "dust" factor had large mass contributions from Al, Fe, and Cu (Figures S4 and S5). Mn, Ni, V, and Cd had higher mass concentrations in fine aerosols than in coarse aerosols. These four metals are known to be consistently found in aerosols from anthropogenic sources such as vehicle and ship emissions, combustion and industrial processes (Chow et al., 2022). Pb, Cr, and Co had mostly similar concentrations in the fine and coarse aerosols. Interestingly, the mass concentrations of Mn and Cr were positively correlated with the mass concentration of Al (R = 0.42 and R = 0.33, respectively), and these correlations were statistically significant (Figure S3). Our PMF analysis apportioned Al to two factors, "dust" and "industrial factor 1", though the Al contribution to "industrial factor 1" was substantially smaller compared to "dust" (Figures S4 and S5). The "dust" factor had a significant Mn contribution, which could explain the strong correlation between the mass concentrations of Al and Mn. Cr was apportioned primarily to "industrial factor 1", which could explain the strong correlation between the mass concentrations of Al and Cr. The mass concentrations of Ni, V, Cd, Pb, and Co showed weak correlations with the mass concentration of Al (Figure S3).

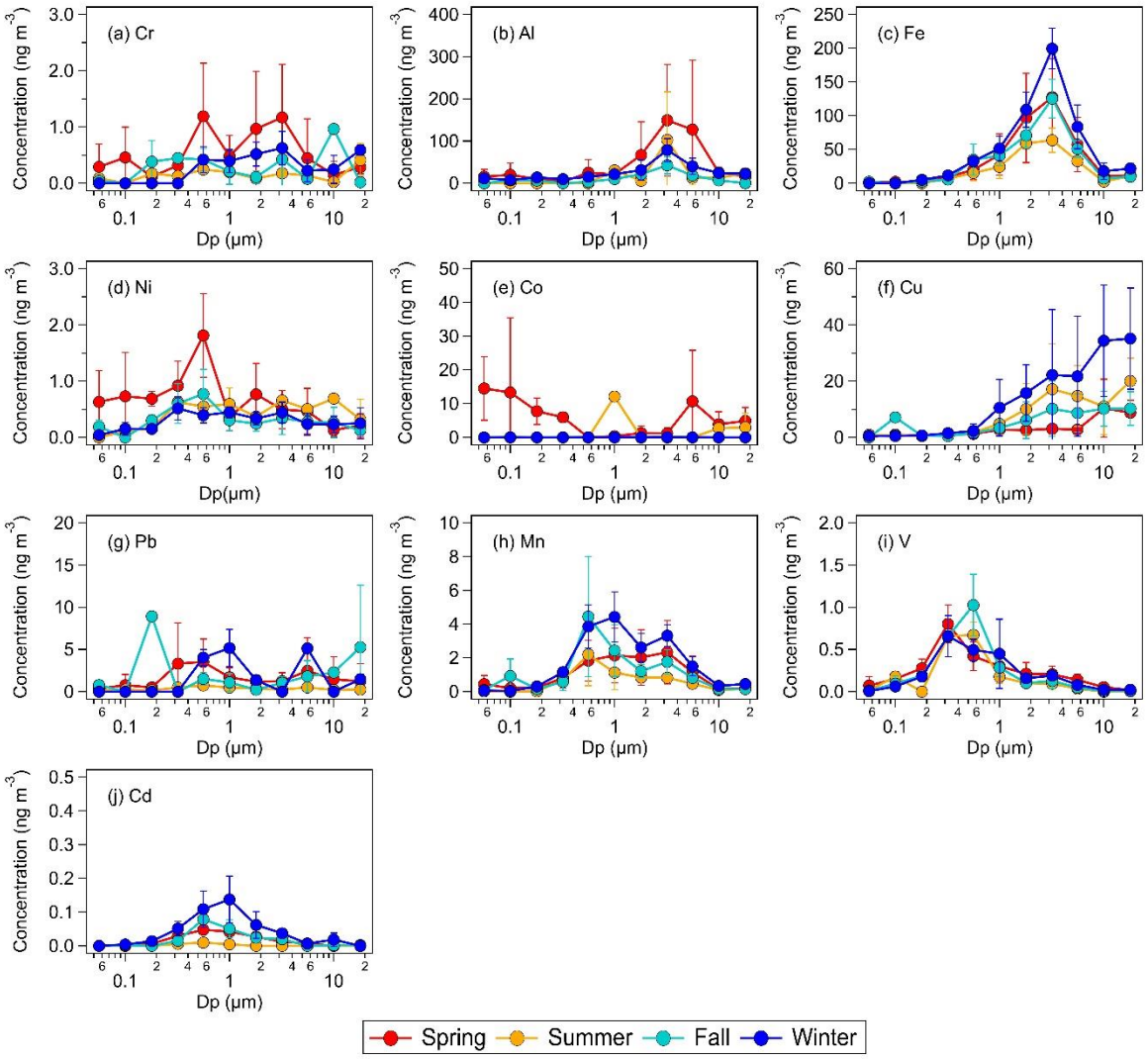

294

295 **Figure 1:** Seasonal average concentrations of total elemental metals in size-fractionated
296 aerosols sampled by the MOUDI with the following nominal cut points (Dp): 0.056 μm (size
297 fraction 1), 0.1 μm (size fraction 2), 0.18 μm (size fraction 3), 0.32 μm (size fraction 4), 0.56
298 μm (size fraction 5), 1.0 μm (size fraction 6), 1.8 μm (size fraction 7), 3.2 μm (size fraction 8),
299 5.6 μm (size fraction 9), 10 μm (size fraction 10), and 18 μm (size fraction 11). The error bars
300 represent one standard deviation of the seasonal average value.

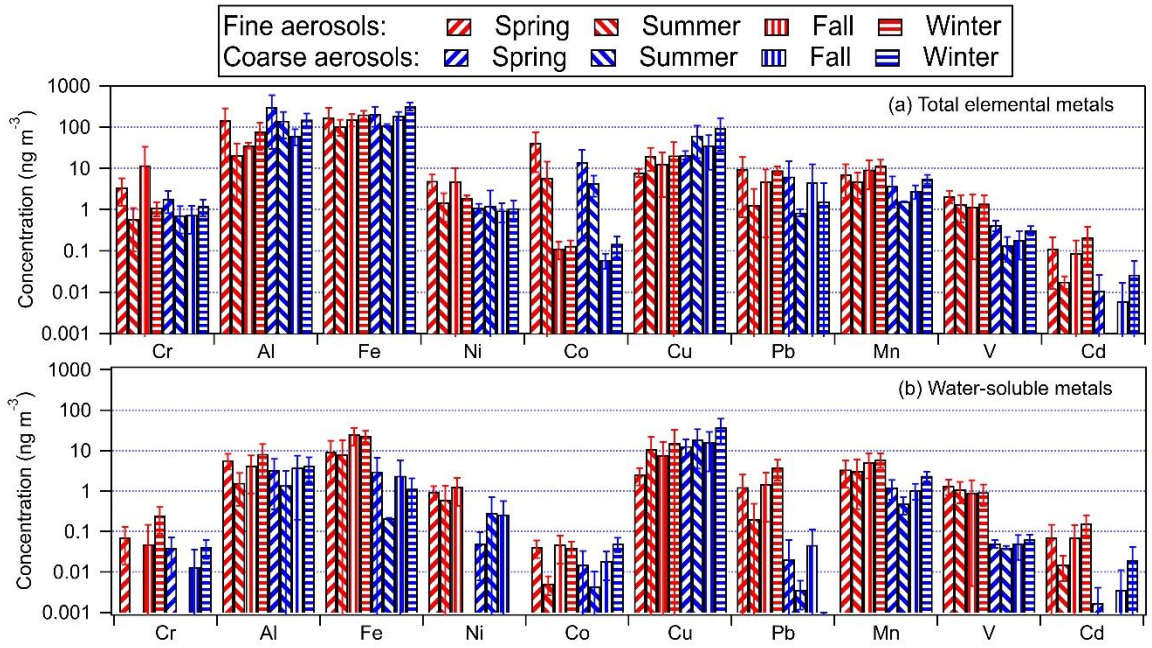

Figure 2: Seasonal average mass concentrations of (a) total metals and (b) water-soluble metals in fine (red) and coarse (blue) aerosols. The error bars represent one standard deviation. The y axes are on logarithm scales.

Jiang et al. (2015) previously measured the mass concentrations of various total metals in $PM_{2.5}$ and $PM_{2.5-10}$ in Kowloon Tong. The authors carried out their measurements from 12 November 2012 to 10 December 2012 (winter) and from 8 April 2013 to 13 May 2013 (spring/summer). To gain some insights into how the aerosol metal concentrations at this urban site have changed since 2012/2013, we compared the average mass concentrations of total metals in fine and coarse aerosols measured in this study to those measured by Jiang et al. (2015). As shown in Table S1, lower mass concentrations were measured in fine (21 % to 93 % lower) and coarse (0.5 % to 92 % lower) aerosols for most of the metals in this study. While the lower aerosol metal mass concentrations could be partly attributed to lower levels of anthropogenic activities in 2021/2022 due to COVID-19, it is likely that the implementation of numerous local and regional air pollution policies to reduce industrial and transport-related emissions over the last decade contributed largely to this decrease. For instance, industrial upgrades resulting from the implementation of the "double transfer" policy (industry and labor transfer away from primary industries) in Guangdong likely caused the decline in the mass concentrations of metals that are typically associated with industrial activities such as Cu and

Mn (Zhong et al., 2013; Chow et al., 2022). In addition, government policies driving the switch to cleaner fuels for energy generation and transport in Hong Kong and the GBA likely caused the decline in the mass concentrations of metals such as Pb, Ni, V, and Fe. Interestingly, higher mass concentrations were measured for Fe and Cu in coarse aerosols in this study compared to those measured by Jiang et al. (2015). Fe and Cu in coarse aerosols have previously been linked to resuspended road dust from brake and tire wear (Garg et al., 2000; Adachi and Tainosho, 2004; Lough et al., 2005). Based on publicly available government data (www.td.gov.hk), the number of registered motor vehicles in Hong Kong has increased by about 34 % over the last decade. It is possible that the higher Fe and Cu mass concentrations in coarse aerosols in this study were due to increased contributions from road dust as a result of increased vehicle fleet size at the urban site.

A PMF source apportionment analysis was performed to determine the major sources of aerosol metals measured in this study (Section S1). A five-factor solution was selected since it gave the most reasonable factor profiles and had high stability. The five factors were broadly classified as “sea salt”, “dust”, “ship emissions”, “industrial factor 1”, and “industrial factor 2” based on the tracer species with the highest mass loadings in each factor (Figure S4). A discussion on how these five factors were classified can be found in Section S1. Figure S5 shows the seasonal mass contributions of each source to each metal species in coarse and fine aerosols. Metals with large fractions in the dust and sea salt source factor profiles generally had higher mass concentrations in coarse aerosols. Conversely, metals with large fractions in the ship emissions and industrial source factor profiles generally had higher mass concentrations in fine aerosols. Higher mass contributions were usually observed in the winter and/or spring seasons, which could be attributed to the long-range transport of polluted air masses by northly prevailing winds from emission sources located in continental areas north of Hong Kong (Figure S1).

3.2. Water-soluble metals

Figure 3 shows the seasonal average mass concentrations of water-soluble metals in size-fractionated aerosols. The size distribution of six of the water-soluble metals (Cr, Fe, Pb,

Mn, V, and Cd) mostly exhibited a single mode, all of which were found in the fine aerosol mode. Fe, Mn, V, and Cd exhibited a single mode for both their total and water-soluble components (Figures 1 and 3). Of these four metals, only the modes of total and water-soluble Fe showed obvious differences, with total Fe exhibiting a mode at around 3.2 μm (size fraction 8) and water-soluble Fe exhibiting a mode at around 0.56 μm to 1.0 μm (size fractions 5 to 6). The modes of total and water-soluble Cu also showed obvious differences. While the mode of total Cu was at ≥18 μm (Figure 1f), the modes of water-soluble Cu were found at substantially small aerosol sizes (Figure 3f).

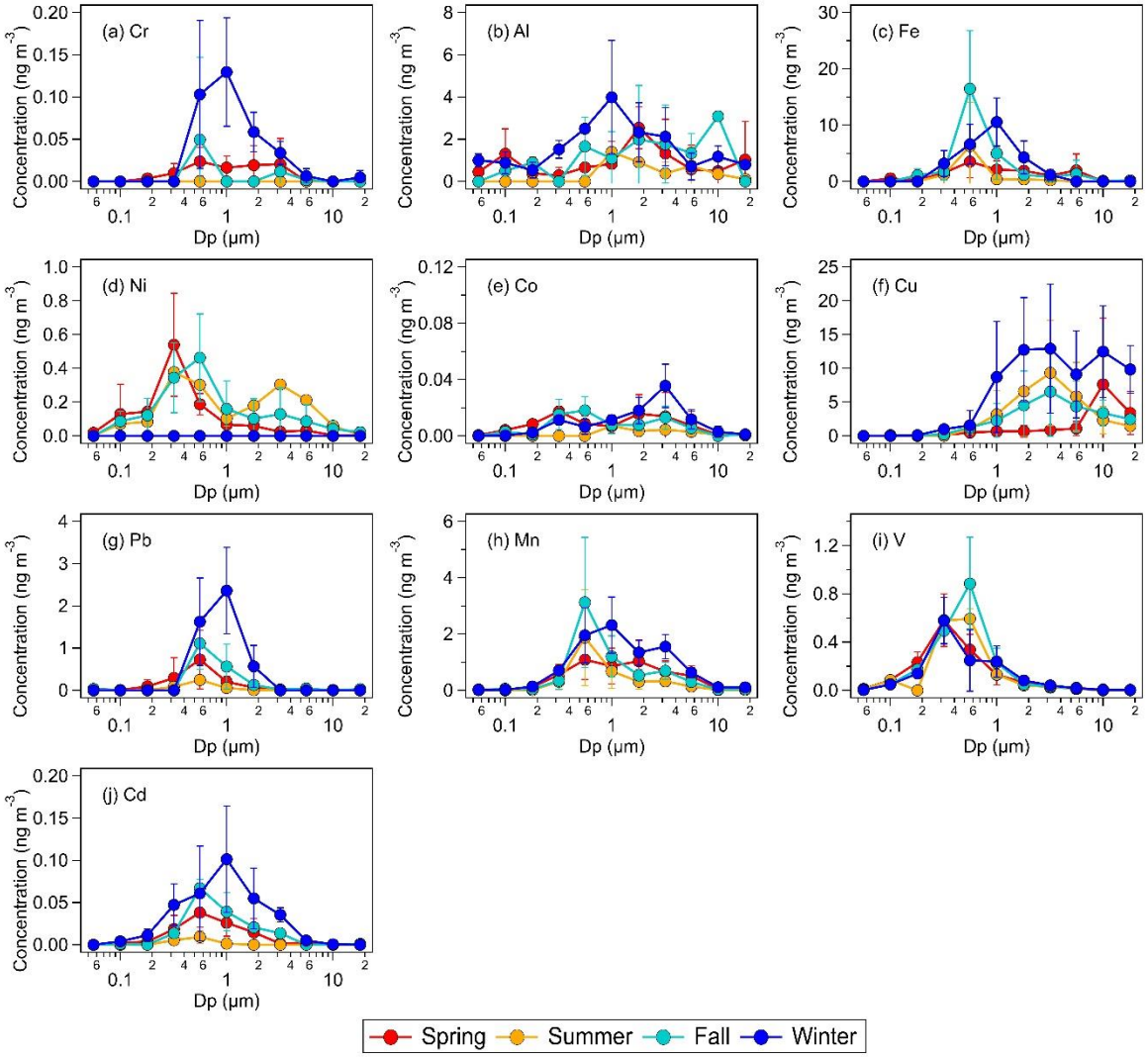

Figure 3: Seasonal average concentrations of water-soluble metals in size-fractionated aerosols sampled by the MOUDI with the following nominal cut points (Dp): 0.056 μm (size fraction 1), 0.1 μm (size fraction 2), 0.18 μm (size fraction 3), 0.32 μm (size fraction 4), 0.56 μm (size

fraction 5), 1.0 μm (size fraction 6), 1.8 μm (size fraction 7), 3.2 μm (size fraction 8), 5.6 μm (size fraction 9), 10 μm (size fraction 10), and 18 μm (size fraction 11). The error bars represent one standard deviation of the seasonal average value.

Figure 2b shows the seasonal average mass concentrations of water-soluble metals in fine and coarse aerosols. Similar to the total metals, higher mass concentrations of water-soluble metals were usually measured during the winter and/or spring seasons. With the exception of Cu, the water-soluble metals usually had higher mass concentrations in fine aerosols than in coarse aerosols. The water-soluble metals generally had the same order of abundance as the total metals with some slight variations. The mass concentrations of water-soluble metals generally correlated with the mass concentrations of total metals (Table S2). This indicated that the water-soluble metals were largely derived from their total metals through atmospheric processing, and/or that water-soluble and water-insoluble metals have the same emission sources. For most of the metals, correlations between the mass concentrations of water-soluble and total metals were higher for fine aerosols than for coarse aerosols. This could be due to enhanced metal dissolution in fine aerosols via acid processing and/or the formation of stable metal-organic complexes, which are two atmospheric chemical processes that play key roles in influencing the solubilities of aerosol metals in many locations. This is because acidic inorganic species that promote acid processing and organic species that can serve as organic ligands are typically present in larger quantities in fine aerosols than in coarse aerosols. It is also possible that differences in metal mineralogy and atmospheric processing mechanisms in fine vs. coarse aerosols could have contributed to differences in the metal dissolution rates (Oakes et al., 2012; Longo et al., 2016; Ingall et al., 2018).

Figure 4 shows the study-averaged fractional solubilities for the ten metals in fine and coarse aerosols. The study-averaged metal fractional solubilities spanned a wide range for both fine (7.8 % to 71.2 %) and coarse (0.4 % to 47.9 %) aerosols. With the exception of Cu, the metals generally exhibited higher fractional solubilities in fine aerosols compared to coarse aerosols. The aerosol size-dependent metal fractional solubility could be explained by differences in the aerosol composition and metal mineralogy, which resulted in different metal dissolution rates and/or mechanisms for aerosols of different sizes. Our observations of mostly

higher metal fractional solubilities in fine aerosols are consistent with previous studies conducted in Hong Kong and other locations worldwide (Baker et al., 2006; Jiang et al., 2014; Jiang et al., 2015; Fang et al., 2017; Gao et al., 2019; Baker et al., 2020; Gao et al., 2020b; Zhang et al., 2022). No season-dependent trend was observed for the metal fractional solubilities.

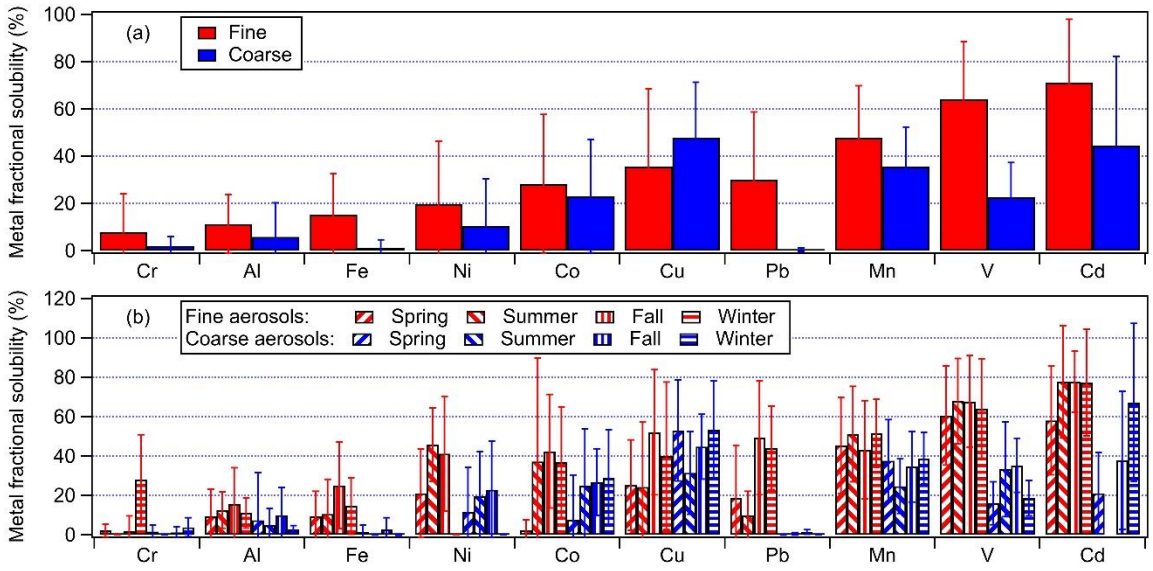

Figure 4: (a) Study-averaged fractional solubilities of metals in fine and coarse aerosols. (b) Seasonal average fractional solubilities of metals in fine and coarse aerosols. The error bars represent one standard deviation.

Some studies have reported that aerosol metal fractional solubilities will exhibit inverse relationships with the total metal concentrations as a result of atmospheric processing (Baker and Jickells, 2006; Sholkovitz et al., 2012; Mahowald et al., 2018; Shelley et al., 2018; Zhang et al., 2022). There was significant scatter in many of our datasets (Figure S6), which made it difficult to discern some of the relationships between the metal fractional solubilities and total metal concentrations. Inverse relationships between the fractional solubility and total metal concentration were noticeable for Cr, Al, Fe, Ni, Cu, Pb, and Mn. However, inverse relationships between the Co, V, and Cd fractional solubilities and their total metal concentrations were less noticeable due to their low concentrations and scatter in their datasets. A number of factors could have contributed to the scatter in the datasets. For instance, the scatter could be a result of the total and water-soluble metal concentrations being substantially

409 different in individual aerosol particles, which would not be captured by the bulk chemical
410 analysis performed in this study (Oakes et al., 2012; Longo et al., 2016; Ingall et al., 2018).
411 The metal dissolution rates in individual aerosol particles could also be significantly different
412 due to differences in metal mineralogy, aerosol acidity levels, presence of organic ligands etc.
413 in individual aerosol particles.

414 **3.3. Factors that control the aerosol metal solubilities**

415 Here, we identify the factors that control metal solubilities in fine aerosols since they
416 are believed to exert higher toxicity than coarse aerosols due to their small sizes. Our analyses
417 focus on aerosol metal dissolution via metal-organic complexation reactions and acid
418 processing, which are two atmospheric chemical processes believed to drive aerosol metal
419 dissolution in most environments. Laboratory studies have shown that the presence of organic
420 ligands enhances Fe dissolution in aerosols (Paris et al., 2011; Chen and Grassian, 2013; Paris
421 and Desboeufs, 2013; Wang et al., 2017). Water-soluble dicarboxylic acids, especially oxalate,
422 form stable complexes with Fe ions, which will lower the energy barrier for Fe dissolution.
423 While evidence of organic ligand-promoted metal dissolution in ambient aerosols has been less
424 conclusive, recent field studies compared the oxalate and water-soluble Fe concentrations to
425 show that the presence of organic ligands could contribute to aerosol Fe solubility. For instance,
426 strong positive correlations between oxalate and water-soluble Fe mass concentrations were
427 observed for $PM_{2.5}$ collected at six urban and rural sites in Canada (Tao and Murphy, 2019).
428 The Fe fractional solubility was also observed to be positively correlated with the molar ratio
429 of oxalate and Fe for $PM_{2.5}$ collected at a suburban site in Qingdao, China (Zhang et al., 2022).

430 To investigate whether organic ligands influenced aerosol metal solubilities in this study,
431 we attempted to measure oxalate in the size-fractionated aerosol samples using IC. However,
432 we could not detect oxalate, which indicated that the concentrations of oxalate (if present) were
433 below the detection limits of our IC instrument. It should be noted that although a recent study
434 reported the copresence of Fe and oxalate in individual aerosol particles at a suburban site in
435 Hong Kong using single particle mass spectrometry (Zhou et al., 2020), organic ligand-
436 promoted metal dissolution is a slow process, and it plays a minor role in metal dissolution

under low pH conditions (Zhu et al., 1993). The fine aerosols collected in this study were mostly acidic, with about 60 % of the calculated pH values being less than 3. This suggested that organic ligand-promoted dissolution may have played a minor role in enhancing aerosol metal solubilities in this study due to the acidic nature of the aerosols.

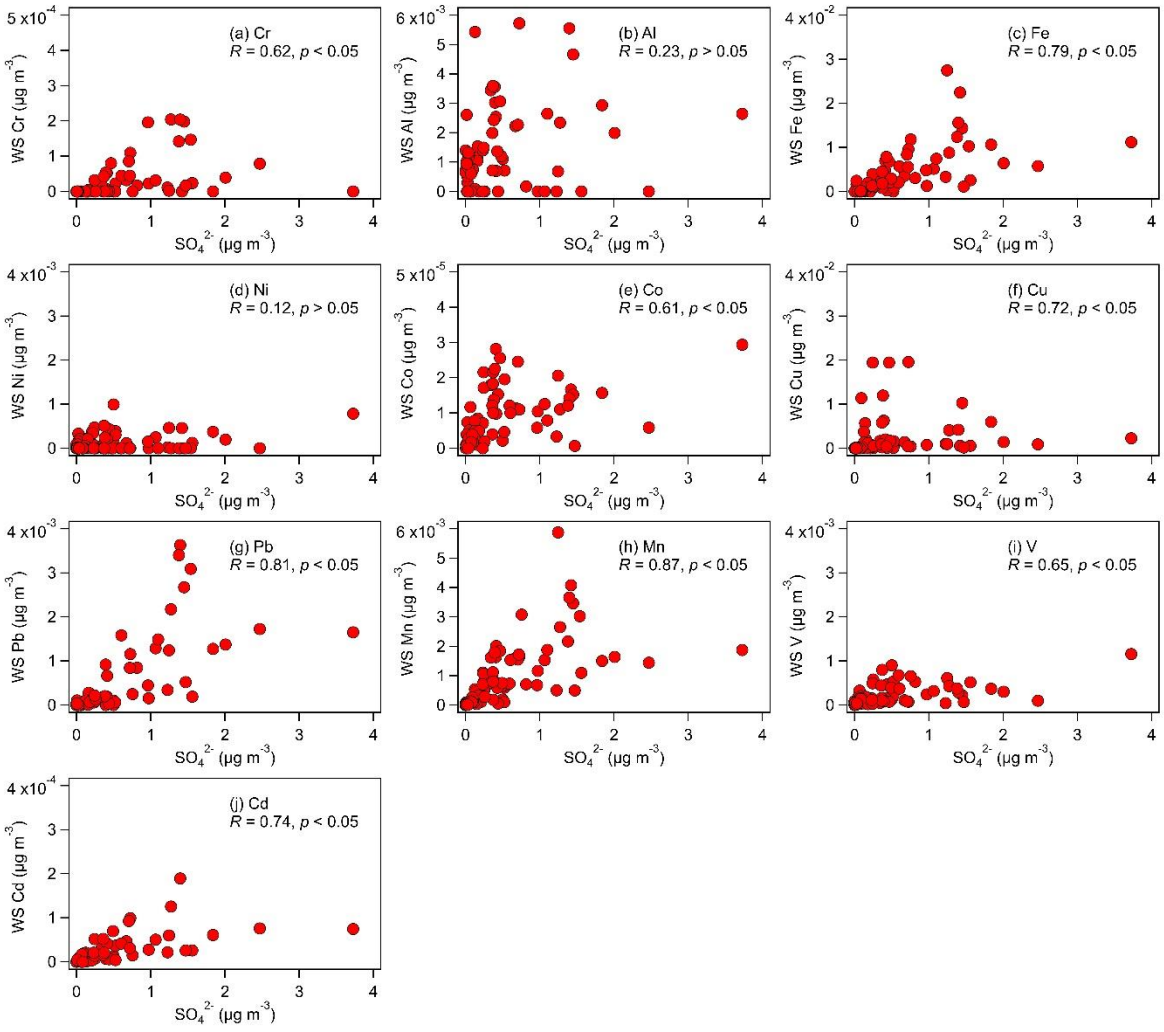

Figure 5: Relationships between the mass concentrations of water-soluble (WS) metals and sulfate in fine aerosols. Only data with non-zero total metal concentrations were used in the figures. Also shown are the spearman correlation coefficients for each relationship.

The acidic nature of the aerosols raises the possibility that acid processing played a major role in enhancing aerosol metal solubilities. A previous study that utilized nanoscale single-particle mass spectrometric and imaging techniques to analyze the mixing states of Fe-containing aerosols collected over the East China Sea provided insights into the mechanism of

Fe dissolution by acidic species that condensed onto atmospheric aerosols (Li et al., 2017). The authors reported that Fe oxide-rich aerosols emitted from steel plants and coal combustion were coated with thick layers of acidic sulfate after 1 to 2 days of atmospheric aging. These sulfate coatings originated from the condensation of sulfuric acid, which were formed from reactions of anthropogenic SO_2. While the fresh aerosols were composed primarily of insoluble Fe oxide, the aged aerosols contained soluble Fe sulfate that were internally mixed in the sulfate coatings. Although the mechanism proposed by Li et al. (2017) focused on explaining how sulfate-driven acid processing leads to the dissolution of the water-insoluble forms Fe, this mechanism likely applies to the other aerosol metals as well. During acid processing, acidic species have to overcome the buffering capacity of the aqueous aerosol particle to raise the aerosol acidity level to the point where the dissolution of metal species is thermodynamically favored. Sulfate was the most abundant aqueous-phase acidic species in our size-fractionated aerosol samples. The concentrations of nitrate (another aqueous-phase acidic species) were very low (about 18 times lower than sulfate, on average), while aqueous-phase organic acids were not detected. Hence, we first analyzed the relationships between the concentrations of water-soluble metals and sulfate. Figure 5 shows that despite the scatter in the datasets, the concentrations of water-soluble metals were positively correlated with the concentration of sulfate, though the correlations between the concentrations of sulfate and water-soluble Al and Ni were not statistically significant. These positive correlations could be due, in part, to the water-soluble metals and sulfate precursor (i.e., SO_2) being emitted from the same sources. However, the masses of primary water-soluble aerosol metals are not known. The positive correlations could also be due to the role that sulfate plays in aerosol metal dissolution during acid processing.

To investigate the roles that sulfate and nitrate played in controlling aerosol metal solubilities, we analyzed the relationships between the metal fractional solubilities and sulfate and nitrate concentrations. In general, the correlations between the metal fractional solubilities and sulfate concentration (Table 1) were substantially higher than the correlations between the metal fractional solubilities and nitrate concentration (Table S3). This implied that sulfate likely plays a more important role than nitrate in controlling aerosol metal solubilities, which is not surprising given the low concentrations of nitrate detected (about 18 times lower than sulfate,

on average). Analyses of the correlations between the metal fractional solubilities and sulfate concentration (Table 1 and Figure 6) indicated that the Cr, Fe, Co, Cu, Pb, and Mn fractional solubilities were positively correlated with the sulfate concentration, and these correlations were statistically significant. This implied that sulfate played a key role in the formation of water-soluble Cr, Fe, Co, Cu, Pb, and Mn, likely though sulfate-driven acid dissolution of their water-insoluble forms. Conversely, the positive correlations between the sulfate concentration and the Al, Ni, V, and Cd fractional solubilities were weak and not statistically significant. Interestingly, the V and Cd fractional solubilities showed weak correlations with the sulfate concentration ($R = 0.14$ and $R = 0.04$, respectively), whereas their water-soluble concentrations showed strong correlations with the sulfate concentration ($R = 0.65$ and $R = 0.74$, respectively). It is possible that the strong correlations of sulfate concentration with water-soluble V and Cd concentrations but not with V and Cd fractional solubilities were due to a large fraction of water-soluble V and Cd having the same sources as sulfate and its precursor (i.e., SO_2). For instance, Celo et al. (2015) reported that substantial concentrations of water-soluble aerosol metals (including V), sulfate, and SO_2 are present in exhaust emissions from the main engines of commercial marine vessels.

Table 1: Spearman rank correlations between the metal fractional solubilities and W_i and H^+_{air} in fine aerosols[a]

Metal	Sulfate	W_i	H^+_{air}	pH
Cr	**0.62**	**0.42**	**0.48**	-0.16
Al	0.14	0.08	0.14	-0.06
Fe	**0.53**	**0.31**	**0.50**	**-0.33**
Ni	0.03	0.01	0.18	**-0.26**
Co	**0.41**	**0.41**	**0.23**	-0.05
Cu	**0.74**	**0.72**	**0.24**	-0.07
Pb	**0.53**	**0.41**	**0.34**	-0.13
Mn	**0.49**	**0.43**	**0.23**	-0.01
V	0.14	0.01	0.21	-0.20
Cd	0.04	0.10	0.13	0.22

[a] Bold: statistically significant ($p < 0.05$)

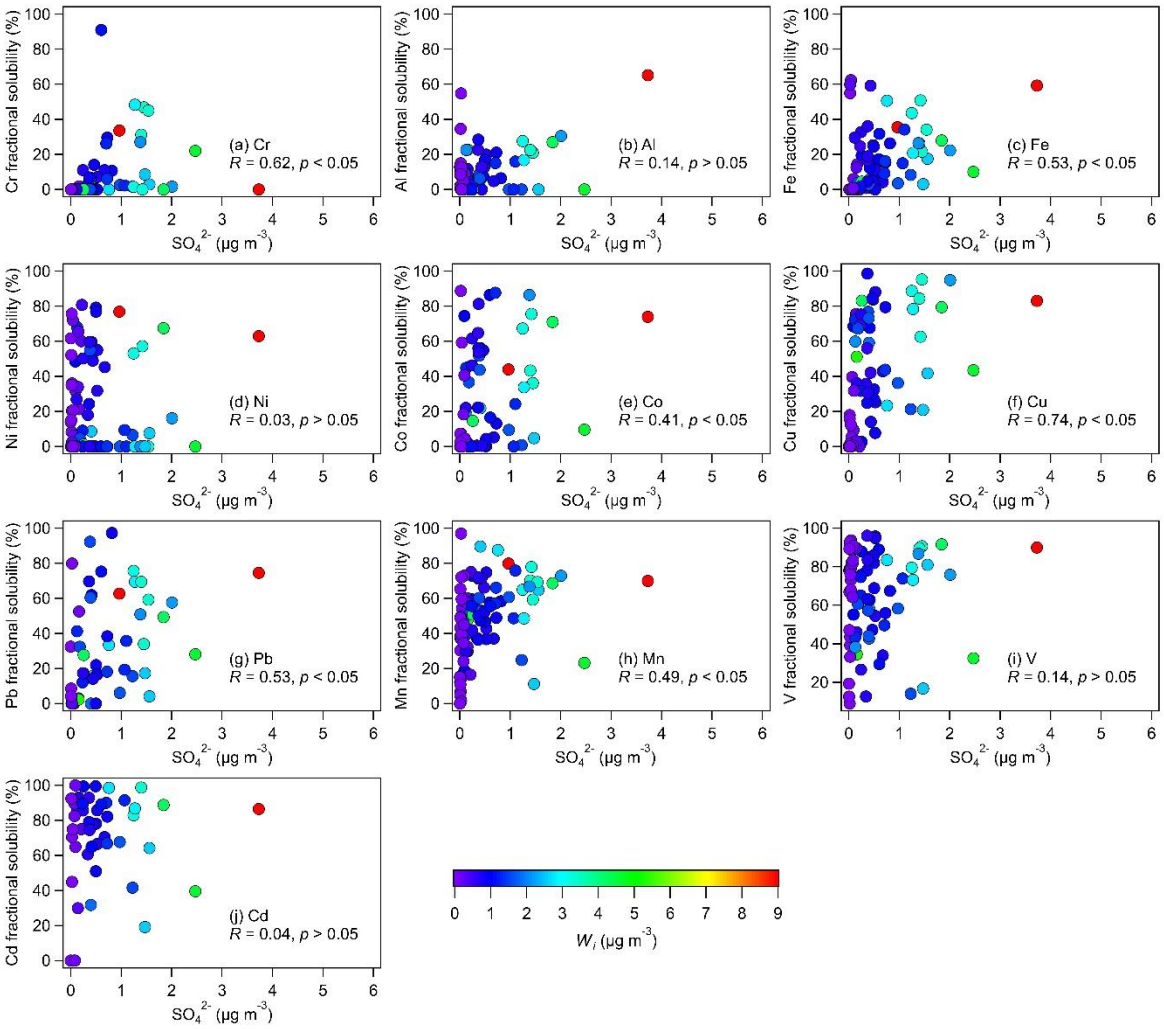

497

498 **Figure 6:** Relationships between the metal fractional solubilities and sulfate mass
499 concentration in fine aerosols. Only data with non-zero total metal concentrations were used in
500 the figures. Also shown are the spearman correlation coefficients for each relationship. The
501 symbols are colored by the corresponding W_i concentrations calculated by ISORROPIA-II.
502 The W_i concentrations increased with sulfate concentrations.

503 High levels of aerosol acidity and liquid water are generally needed for the acid
504 dissolution of metals in an aqueous aerosol particle. In addition to being the main contributor
505 to aerosol acidity levels (i.e., H^+_{air}), sulfate is a highly hygroscopic species that will influence
506 the overall aerosol water uptake behavior, which will drive W_i. Sulfate was the main driver of
507 W_i in fine aerosols in our study since the mass concentrations of nitrate (another highly
508 hygroscopic species) were very low (about 18 times lower than sulfate, on average). Both W_i
509 and H^+_{air} were controlled primarily by sulfate (sulfate and W_i R = 0.90, p < 0.05; sulfate and

H^+_{air} R = 0.63, p < 0.05). Thus, we analyzed the relationships between the aerosol metal fractional solubilities and W_i and H^+_{air} (Figures S7 and S8). Table 1 shows that correlations between the Al, Ni, V, and Cd fractional solubilities and W_i and H^+_{air} were weak. Together, the weak correlations between the fractional solubilities of Al, Ni, V, and Cd and sulfate, W_i, and H^+_{air} implied that acid processing may have played a minor role in enhancing the solubilities of these four metals. Other atmospheric processes beyond acid processing (e.g., cloud processing, photoreduction) could have played more important roles in enhancing the solubilities of these four metals (Zhu et al., 1993; Spokes et al., 1994; Kuma et al., 1995). It is possible that these four metals had slow acid dissolution rates as a result of their mineralogy and oxidation states. The impacts of mineralogy and oxidation states on the susceptibilities of water-insoluble Al, Ni, V, and Cd to acid dissolution are currently not known. However, previous studies showed that different aerosol Fe mineralogy and oxidation states have different susceptibilities to acid dissolution that will occur at different timescales (Ingall et al., 2018). Hence, analogous to Fe, it is possible that the mineralogy and oxidation states of Al, Ni, V, and Cd in the collected aerosols may have resulted in these four metals being less susceptible to acid processing, which in turn caused them to undergo slow sulfate-driven acid dissolution from water-insoluble forms to water-soluble forms.

Table 1 shows that the Cr, Fe, Co, Cu, Pb, and Mn fractional solubilities were positively correlated with W_i and H^+_{air}, and these correlations were statistically significant. Together, the statistically significant positive correlations between the fractional solubilities of Cr, Fe, Co, Cu, Pb, and Mn and sulfate, W_i, and H^+_{air} indicated that acid processing likely played an important role in enhancing the solubilities of these six metals. The fractional solubilities of Co, Cu, Pb, and Mn were more strongly correlated with the W_i concentration than with the H^+_{air} concentration. This suggested that W_i had a stronger influence on the acid dissolution of Co, Cu, Pb, and Mn. The strong influence that W_i has on the metal fractional solubility could be explained by the role of aerosol water as a reaction medium for the acid dissolution of metals in an aqueous aerosol particle. Wong et al. (2020) previously showed that at a relatively constant aerosol pH, a decrease in W_i will lead to a decrease in the reaction medium volume, which in turn will lead to decreases in the overall formation rates of water-soluble metals.

539 Conversely, the fractional solubilities of Cr and Fe were more strongly correlated with the H^+_{air}
540 concentration than with the W_i concentration. This suggested that the aerosol acidity levels had
541 a stronger influence on the acid dissolution of Cr and Fe. Despite the statistically significant
542 positive correlations between the fractional solubilities of Cr, Fe, Co, Cu, Pb, and Mn and
543 sulfate, W_i, and H^+_{air} (Table 1), there was significant scatter in the datasets (Figures 6, S7, and
544 S8). This scatter could be a result of the sulfate, W_i, H^+_{air}, total and water-soluble metal
545 concentrations being substantially different in individual aerosol particles, which would not be
546 captured by the bulk chemical analysis and thermodynamic modeling performed in this study.
547 The metal dissolution rates in individual aerosol particles could also be significantly different
548 due to differences in metal mineralogy, aerosol acidity levels, etc. in individual aerosol particles.
549 In addition, a recent study by Yang et al. (2021) reported that the filterable metal fractions in
550 the water extracts may contain some metals in water-insoluble forms with small diameters that
551 allowed them to pass through the pores of syringe filters. This would result in over-estimated
552 metal fractional solubilities, which could explain why some of the data points in Figure 6
553 showed high metal fractional solubilities at low sulfate concentrations.

554 Interestingly, variability in the aerosol pH did not appear to be a key driver of the
555 variability in the solubilities of Cr, Fe, Co, Cu, Pb, and Mn. It was difficult to discern aerosol
556 pH-dependent fractional solubility trends for these six metals, and their fractional solubilities
557 were not highly correlated with aerosol pH (Table 1 and Figure S9). This could be attributed
558 partly to the scatter in the datasets caused by differences in the metal solubilities and pH in
559 individual aerosol particles that would not be captured by the bulk chemical analysis and
560 thermodynamic modeling performed in this study. The absence of obvious aerosol pH-
561 dependent fractional solubility trends could also be due to the insensitivity of aerosol pH to the
562 variability of sulfate ($R = -0.22$, $p < 0.05$). Based on Equation (1), the aerosol pH could be
563 viewed simply as the ratio of H^+_{air} and W_i. Both W_i and H^+_{air} were highly variable in this study,
564 and both were controlled primarily by sulfate. As a result, the ratio of H^+_{air} and W_i, or the
565 aerosol pH, would be fairly insensitive to sulfate even though it was driven primarily by sulfate.
566 Previous studies have similarly reported weak or the absence of aerosol pH-dependent metal
567 fractional solubility trends despite evidence of aerosol metal dissolution being enhanced by

acid processing (Shi et al., 2020; Wong et al., 2020).

4. Conclusions

In this study, we investigated the abundance and fractional solubilities of ten metals (Fe, Cu, Al, V, Cr, Mn, Co, Ni, Cd, and Pb) in size-fractionated aerosols collected at an urban site in Hong Kong. Weekly aerosol samples were collected for a month during different seasons from March 2021 to January 2022. The main objective of this study was to identify the key factors that controlled metal solubilities in fine aerosols, with a focus on aerosol metal dissolution via the acid processing and metal-organic complexation mechanisms. Hence, other aerosol chemical species were measured in addition to the total and water-soluble metals.

Higher mass concentrations of total metals were usually measured during the winter and/or spring seasons. This was likely due to the long-range transport of polluted air masses by northly prevailing winds from emission sources located in continental areas north of Hong Kong. The total metals could be arranged in the following order based on their abundances: Fe > Al > Cu > Co > Mn > Pb > Cr > Ni > V > Cd. This order of abundance was the same for both fine and coarse aerosols. The major sources of the total metals were sea salt, dust, ship emissions, and industrial activities. Higher mass concentrations of water-soluble metals were also usually measured during the winter and/or spring seasons. With the exception of Cu, the water-soluble metals had higher mass concentrations in fine aerosols than in coarse aerosols. The mass concentrations of water-soluble metals generally correlated with the mass concentrations of total metals, which implied that the water-soluble metals were largely derived from their total metals through atmospheric processing and/or that water-soluble and water-insoluble metals have the same emission sources. The study-averaged metal fractional solubilities spanned a wide range for both fine (7.8 % to 71.2 %) and coarse (0.4 % to 47.9 %) aerosols. With the exception of Cu and Co, the metals exhibited higher fractional solubilities in fine aerosols compared to coarse aerosols. The aerosol size-dependent metal fractional solubility could potentially be attributed to differences in the composition and metal mineralogy which resulted in different metal dissolution rates and/or mechanisms for aerosols of different sizes.

The fine aerosols collected in this study were mostly acidic, with about 60 % of the calculated pH values below 3. The acidic nature of the fine aerosols combined with oxalate (which forms metal-organic complexes easily) not being detected in our aerosol samples suggested that organic ligand-promoted dissolution likely played a minor role in enhancing aerosol metal solubilities. This is because organic ligand-promoted metal dissolution is a slow process, and it plays a minor role in metal dissolution under low pH conditions. Our analyses showed that sulfate, which is the dominant fine aerosol acidic species, exhibited statistically significant positive correlations with both the water-soluble concentrations of Cr, Fe, Co, Cu, Pb, and Mn and their fractional solubilities. In addition, sulfate controlled W_i and H^+_{air}, both of which are needed for acid dissolution of metals in an aqueous aerosol particle. The water-soluble concentrations of Cr, Fe, Co, Cu, Pb, and Mn and their fractional solubilities exhibited statistically significant positive correlations with both W_i and H^+_{air}. Together, the statistically significant positive correlations between the fractional solubilities of Cr, Fe, Co, Cu, Pb, and Mn and sulfate, W_i, and H^+_{air} indicated that acid processing likely played an important role in enhancing the solubilities of these six metals. The fractional solubilities of Co, Cu, Pb, and Mn were more strongly correlated with the W_i concentration than with the H^+_{air} concentration, which implied that W_i had a stronger influence on the acid dissolution of these four metals. The fractional solubilities of Cr and Fe were more strongly correlated with the H^+_{air} concentration than with the W_i concentration, which implied that the aerosol acidity levels had a stronger influence on the acid dissolution of these two metals. Conversely, our analyses suggested that acid processing played a minor role in enhancing the solubilities of Al, Ni, V, and Cd. It is possible that the mineralogy and oxidation states of these four metals made them less susceptible to acid processing.

In conclusion, this study highlights the key role that sulfate plays in controlling the solubilities of a host of metals in fine aerosols (in this case, Cr, Fe, Co, Cu, Pb, and Mn). This is mostly due to sulfate's ability to both strongly acidify the aerosol particle and provide the liquid reaction medium needed for the acid dissolution of metals. Although this study was performed at an urban site in Hong Kong, we expect our findings to broadly apply to other urban areas in Hong Kong and South China, where sulfate is the dominant acidic and

hygroscopic component in fine aerosols. Results from this study can also provide insights into how the solubilities of different aerosol metals will change with the decrease in sulfate as Hong Kong and other cities in South China transition away from coal combustion as their main energy source to improve local and regional air quality and combat climate change.

Data availability: The data used in this publication is available to the community and can be accessed at: https://doi.org/10.5281/zenodo.7013770 (Yang et al., 2022).

Author contributions: J.Y. and T.N. designed the study. J.Y. collected the field samples. J.Y., L.M., and W.C.A. performed chemical analysis of the field samples. J.Y., X.H., Y.M., and T.N. analyzed the data. J.Y. and T.N. prepared the manuscript with contributions from all co-authors.

Competing interests: One of the authors is a member of the editorial board of *Atmospheric Chemistry and Physics*. The peer-review process was guided by an independent editor, and the authors also have no other competing interests to declare.

Acknowledgements: This work was supported by the Research Grants Council of Hong Kong (project number 21304919).

References

Adachi, K. and Tainosho, Y.: Characterization of heavy metal particles embedded in tire dust, Environment International, 30, 1009-1017, https://doi.org/10.1016/j.envint.2004.04.004, 2004.

Al-Abadleh, H. A.: Review of the bulk and surface chemistry of iron in atmospherically relevant systems containing humic-like substances, Rsc Advances, 5, 45785-45811, https://doi.org/10.1039/c5ra03132j, 2015.

Al-Abadleh, H. A.: Aging of atmospheric aerosols and the role of iron in catalyzing brown carbon formation, Environmental Science: Atmospheres, 1, 297-345, 10.1039/D1EA00038A, 2021.

Baker, A. R. and Jickells, T. D.: Mineral particle size as a control on aerosol iron solubility, Geophysical Research Letters, 33, https://doi.org/10.1029/2006GL026557, 2006.

Baker, A. R., Li, M., and Chance, R.: Trace Metal Fractional Solubility in Size-Segregated Aerosols From the Tropical Eastern Atlantic Ocean, Global Biogeochemical Cycles, 34, e2019GB006510, https://doi.org/10.1029/2019GB006510, 2020.

Baker, A. R., Jickells, T. D., Witt, M., and Linge, K. L.: Trends in the solubility of iron,

654 aluminium, manganese and phosphorus in aerosol collected over the Atlantic Ocean, Marine
655 Chemistry, 98, 43-58, https://doi.org/10.1016/j.marchem.2005.06.004, 2006.

656 Bates, J. T., Fang, T., Verma, V., Zeng, L. H., Weber, R. J., Tolbert, P. E., Abrams, J. Y., Sarnat,
657 S. E., Klein, M., Mulholland, J. A., and Russell, A. G.: Review of Acellular Assays of Ambient
658 Particulate Matter Oxidative Potential: Methods and Relationships with Composition, Sources,
659 and Health Effects, Environmental Science & Technology, 53, 4003-4019,
660 https://doi.org/10.1021/acs.est.8b03430, 2019.

661 Birmili, W., Allen, A. G., Bary, F., and Harrison, R. M.: Trace Metal Concentrations and Water
662 Solubility in Size-Fractionated Atmospheric Particles and Influence of Road Traffic,
663 Environmental Science & Technology, 40, 1144-1153, https://doi.org/10.1021/es0486925,
664 2006.

665 Boyd, P. W., Jickells, T., Law, C. S., Blain, S., Boyle, E. A., Buesseler, K. O., Coale, K. H.,
666 Cullen, J. J., de Baar, H. J. W., Follows, M., Harvey, M., Lancelot, C., Levasseur, M., Owens,
667 N. P. J., Pollard, R., Rivkin, R. B., Sarmiento, J., Schoemann, V., Smetacek, V., Takeda, S.,
668 Tsuda, A., Turner, S., and Watson, A. J.: Mesoscale iron enrichment experiments 1993-2005:
669 Synthesis and future directions, Science, 315, 612-617,
670 https://doi.org/10.1126/science.1131669, 2007.

671 Bresgen, N. and Eckl, P. M.: Oxidative stress and the homeodynamics of iron metabolism,
672 Biomolecules, 5, 808-847, https://doi.org/10.3390/biom5020808, 2015.

673 Brook, R. D., Rajagopalan, S., Pope, C. A., Brook, J. R., Bhatnagar, A., Diez-Roux, A. V.,
674 Holguin, F., Hong, Y. L., Luepker, R. V., Mittleman, M. A., Peters, A., Siscovick, D., Smith, S.
675 C., Whitsel, L., Kaufman, J. D., Amer Heart Assoc Council, E., Council Kidney Cardiovasc,
676 D., and Council Nutr Phys Activity, M.: Particulate Matter Air Pollution and Cardiovascular
677 Disease An Update to the Scientific Statement From the American Heart Association,
678 Circulation, 121, 2331-2378, https://doi.org/10.1161/CIR.0b013e3181dbece1, 2010.

679 Celo, V., Dabek-Zlotorzynska, E., and McCurdy, M.: Chemical Characterization of Exhaust
680 Emissions from Selected Canadian Marine Vessels: The Case of Trace Metals and Lanthanoids,
681 Environmental Science & Technology, 49, 5220-5226, https://doi.org/10.1021/acs.est.5b00127,
682 2015.

683 Chen, H. H. and Grassian, V. H.: Iron Dissolution of Dust Source Materials during Simulated
684 Acidic Processing: The Effect of Sulfuric, Acetic, and Oxalic Acids, Environmental Science &
685 Technology, 47, 10312-10321, https://doi.org/10.1021/es401285s, 2013.

686 Cheng, Y., Lee, S. C., Cao, J., Ho, K. F., Chow, J., Watson, J., and Ao, C.: Elemental
687 composition of airborne aerosols at a traffic site and a suburban site in Hong Kong,
688 International Journal of Environment and Pollution, 36, 166-179, 2009.

689 Chow, W. S., Huang, X. H. H., Leung, K. F., Huang, L., Wu, X., and Yu, J. Z.: Molecular and
690 elemental marker-based source apportionment of fine particulate matter at six sites in Hong

691 Kong, China, Science of The Total Environment, 813, 152652,
692 https://doi.org/10.1016/j.scitotenv.2021.152652, 2022.

693 Chu, B., Hao, J., Li, J., Takekawa, H., Wang, K., and Jiang, J.: Effects of two transition metal
694 sulfate salts on secondary organic aerosol formation in toluene/NOxphotooxidation, Frontiers
695 of Environmental Science & Engineering, 7, 1-9, https://doi.org/10.1007/s11783-012-0476-x,
696 2013.

697 Chu, B., Liggio, J., Liu, Y., He, H., Takekawa, H., Li, S.-M., and Hao, J.: Influence of metal-
698 mediated aerosol-phase oxidation on secondary organic aerosol formation from the ozonolysis
699 and OH-oxidation of α-pinene, Scientific Reports, 7, 40311, https://doi.org/10.1038/srep40311,
700 2017.

701 Cohen, A. J., Brauer, M., Burnett, R., Anderson, H. R., Frostad, J., Estep, K., Balakrishnan, K.,
702 Brunekreef, B., Dandona, L., Dandona, R., Feigin, V., Freedman, G., Hubbell, B., Jobling, A.,
703 Kan, H., Knibbs, L., Liu, Y., Martin, R., Morawska, L., Pope, C. A., Shin, H., Straif, K.,
704 Shaddick, G., Thomas, M., van Dingenen, R., van Donkelaar, A., Vos, T., Murray, C. J. L., and
705 Forouzanfar, M. H.: Estimates and 25-year trends of the global burden of disease attributable
706 to ambient air pollution: an analysis of data from the Global Burden of Diseases Study 2015,
707 Lancet, 389, 1907-1918, https://doi.org/10.1016/s0140-6736(17)30505-6, 2017.

708 Costa, D. L. and Dreher, K. L.: Bioavailable transition metals in particulate matter mediate
709 cardiopulmonary injury in healthy and compromised animal models, Environmental Health
710 Perspectives, 105, 1053-1060, https://doi.org/10.2307/3433509, 1997a.

711 Costa, D. L. and Dreher, K. L.: Bioavailable transition metals in particulate matter mediate
712 cardiopulmonary injury in healthy and compromised animal models, Environmental Health
713 Perspectives, 105, 1053-1060, https://doi.org/10.1289/ehp.97105s51053, 1997b.

714 de Baar, H. J. W., Boyd, P. W., Coale, K. H., Landry, M. R., Tsuda, A., Assmy, P., Bakker, D.
715 C. E., Bozec, Y., Barber, R. T., Brzezinski, M. A., Buesseler, K. O., Boye, M., Croot, P. L.,
716 Gervais, F., Gorbunov, M. Y., Harrison, P. J., Hiscock, W. T., Laan, P., Lancelot, C., Law, C. S.,
717 Levasseur, M., Marchetti, A., Millero, F. J., Nishioka, J., Nojiri, Y., van Oijen, T., Riebesell, U.,
718 Rijkenberg, M. J. A., Saito, H., Takeda, S., Timmermans, K. R., Veldhuis, M. J. W., Waite, A.
719 M., and Wong, C. S.: Synthesis of iron fertilization experiments: From the iron age in the age
720 of enlightenment, Journal of Geophysical Research-Oceans, 110,
721 https://doi.org/10.1029/2004jc002601, 2005.

722 Deguillaume, L., Leriche, M., Desboeufs, K., Mailhot, G., George, C., and Chaumerliac, N.:
723 Transition Metals in Atmospheric Liquid Phases: Sources, Reactivity, and Sensitive
724 Parameters, Chemical Reviews, 105, 3388-3431, https://doi.org/10.1021/cr040649c, 2005.

725 Fang, T., Guo, H., Verma, V., Peltier, R. E., and Weber, R. J.: PM2.5 water-soluble elements in
726 the southeastern United States: automated analytical method development, spatiotemporal
727 distributions, source apportionment, and implications for heath studies, Atmos. Chem. Phys.,
728 15, 11667-11682, https://doi.org/10.5194/acp-15-11667-2015, 2015.

729 Fang, T., Guo, H., Zeng, L., Verma, V., Nenes, A., and Weber, R. J.: Highly Acidic Ambient
730 Particles, Soluble Metals, and Oxidative Potential: A Link between Sulfate and Aerosol
731 Toxicity, Environmental Science & Technology, 51, 2611-2620,
732 https://doi.org/10.1021/acs.est.6b06151, 2017.

733 Fountoukis, C. and Nenes, A.: ISORROPIA II: a computationally efficient thermodynamic
734 equilibrium model for K+–Ca2+–Mg2+–NH4+–Na+–SO42−–NO3−–Cl−–H2O aerosols,
735 Atmos. Chem. Phys., 7, 4639-4659, https://doi.org/10.5194/acp-7-4639-2007, 2007.

736 Fountoukis, C., Nenes, A., Sullivan, A., Weber, R., Van Reken, T., Fischer, M., Matias, E.,
737 Moya, M., Farmer, D., and Cohen, R. C.: Thermodynamic characterization of Mexico City
738 aerosol during MILAGRO 2006, Atmospheric Chemistry and Physics, 9, 2141-2156,
739 https://doi.org/10.5194/acp-9-2141-2009, 2009.

740 Frampton, M. W., Ghio, A. J., Samet, J. M., Carson, J. L., Carter, J. D., and Devlin, R. B.:
741 Effects of aqueous extracts of PM10 filters from the Utah Valley on human airway epithelial
742 cells, American Journal of Physiology-Lung Cellular and Molecular Physiology, 277, L960-
743 L967, https://doi.org/10.1152/ajplung.1999.277.5.L960, 1999.

744 Gao, D., Mulholland, J. A., Russell, A. G., and Weber, R. J.: Characterization of water-insoluble
745 oxidative potential of PM2.5 using the dithiothreitol assay, Atmospheric Environment, 224,
746 https://doi.org/10.1016/j.atmosenv.2020.117327, 2020a.

747 Gao, Y., Yu, S., Sherrell, R. M., Fan, S., Bu, K., and Anderson, J. R.: Particle-Size Distributions
748 and Solubility of Aerosol Iron Over the Antarctic Peninsula During Austral Summer, Journal
749 of Geophysical Research: Atmospheres, 125, e2019JD032082,
750 https://doi.org/10.1029/2019JD032082, 2020b.

751 Gao, Y., Marsay, C. M., Yu, S., Fan, S., Mukherjee, P., Buck, C. S., and Landing, W. M.:
752 Particle-Size Variability of Aerosol Iron and Impact on Iron Solubility and Dry Deposition
753 Fluxes to the Arctic Ocean, Scientific Reports, 9, 16653, https://doi.org/10.1038/s41598-019-
754 52468-z, 2019.

755 Garg, B. D., Cadle, S. H., Mulawa, P. A., Groblicki, P. J., Laroo, C., and Parr, G. A.: Brake
756 Wear Particulate Matter Emissions, Environmental Science & Technology, 34, 4463-4469,
757 https://doi.org/10.1021/es001108h, 2000.

758 Garrett, R. G.: Natural Sources of Metals to the Environment, Human and Ecological Risk
759 Assessment: An International Journal, 6, 945-963,
760 https://doi.org/10.1080/10807030091124383, 2000.

761 Giorio, C., D'Aronco, S., Di Marco, V., Badocco, D., Battaglia, F., Soldà, L., Pastore, P., and
762 Tapparo, A.: Emerging investigator series: aqueous-phase processing of atmospheric aerosol
763 influences dissolution kinetics of metal ions in an urban background site in the Po Valley,
764 Environmental Science: Processes & Impacts, 24, 884-897,
765 http://dx.doi.org/10.1039/D2EM00023G, 2022.

He, X., Liu, P., Zhao, W., Xu, H., Zhang, R., and Shen, Z.: Size distribution of water-soluble metals in atmospheric particles in Xi'an, China: Seasonal variations, bioavailability, and health risk assessment, Atmospheric Pollution Research, 12, 101090, https://doi.org/10.1016/j.apr.2021.101090, 2021.

Heal, M. R., Elton, R. A., Hibbs, L. R., Agius, R. M., and Beverland, I. J.: A time-series study of the health effects of water-soluble and total-extractable metal content of airborne particulate matter, Occupational and Environmental Medicine, 66, 636-638, https://doi.org/10.1136/oem.2008.045310, 2009.

Hopke, P. K., Lamb, R. E., and Natusch, D. F. S.: Multielemental characterization of urban roadway dust, Environmental Science & Technology, 14, 164-172, https://doi.org/10.1021/es60162a006, 1980.

Ingall, E. D., Feng, Y., Longo, A. F., Lai, B., Shelley, R. U., Landing, W. M., Morton, P. L., Nenes, A., Mihalopoulos, N., Violaki, K., Gao, Y., Sahai, S., and Castorina, E.: Enhanced Iron Solubility at Low pH in Global Aerosols, Atmosphere, 9, 201, 2018.

Jiang, S. Y., Kaul, D. S., Yang, F., Sun, L., and Ning, Z.: Source apportionment and water solubility of metals in size segregated particles in urban environments, Science of The Total Environment, 533, 347-355, https://doi.org/10.1016/j.scitotenv.2015.06.146, 2015.

Jiang, S. Y. N., Yang, F., Chan, K. L., and Ning, Z.: Water solubility of metals in coarse PM and PM2.5 in typical urban environment in Hong Kong, Atmospheric Pollution Research, 5, 236-244, https://doi.org/10.5094/APR.2014.029, 2014.

Jordi, A., Basterretxea, G., Tovar-Sanchez, A., Alastuey, A., and Querol, X.: Copper aerosols inhibit phytoplankton growth in the Mediterranean Sea, Proceedings of the National Academy of Sciences of the United States of America, 109, 21246-21249, https://doi.org/10.1073/pnas.1207567110, 2012.

Kuma, K., Nakabayashi, S., and Matsunaga, K.: Photoreduction of Fe(III) by hydroxycarboxylic acids in seawater, Water Research, 29, 1559-1569, https://doi.org/10.1016/0043-1354(94)00289-J, 1995.

Lakey, P. S. J., Berkemeier, T., Tong, H. J., Arangio, A. M., Lucas, K., Poschl, U., and Shiraiwa, M.: Chemical exposure-response relationship between air pollutants and reactive oxygen species in the human respiratory tract, Scientific Reports, 6, https://doi.org/10.1038/srep32916, 2016.

Lee, C. S. L., Li, X.-D., Zhang, G., Li, J., Ding, A.-J., and Wang, T.: Heavy metals and Pb isotopic composition of aerosols in urban and suburban areas of Hong Kong and Guangzhou, South China—Evidence of the long-range transport of air contaminants, Atmospheric Environment, 41, 432-447, https://doi.org/10.1016/j.atmosenv.2006.07.035, 2007.

Li, W., Wang, T., Zhou, S., Lee, S., Huang, Y., Gao, Y., and Wang, W.: Microscopic Observation

of Metal-Containing Particles from Chinese Continental Outflow Observed from a Non-Industrial Site, Environmental Science & Technology, 47, 9124-9131, https://doi.org/10.1021/es400109q, 2013.

Li, W., Xu, L., Liu, X., Zhang, J., Lin, Y., Yao, X., Gao, H., Zhang, D., Chen, J., Wang, W., Harrison, R. M., Zhang, X., Shao, L., Fu, P., Nenes, A., and Shi, Z.: Air pollution–aerosol interactions produce more bioavailable iron for ocean ecosystems, Science Advances, 3, e1601749, https://doi.org/10.1126/sciadv.1601749, 2017.

Lippmann, M.: Toxicological and epidemiological studies of cardiovascular effects of ambient air fine particulate matter (PM2.5) and its chemical components: Coherence and public health implications, Critical Reviews in Toxicology, 44, 299-347, https://doi.org/10.3109/10408444.2013.861796, 2014.

Longo, A. F., Feng, Y., Lai, B., Landing, W. M., Shelley, R. U., Nenes, A., Mihalopoulos, N., Violaki, K., and Ingall, E. D.: Influence of Atmospheric Processes on the Solubility and Composition of Iron in Saharan Dust, Environmental Science & Technology, 50, 6912-6920, https://doi.org/10.1021/acs.est.6b02605, 2016.

Lough, G. C., Schauer, J. J., Park, J.-S., Shafer, M. M., DeMinter, J. T., and Weinstein, J. P.: Emissions of Metals Associated with Motor Vehicle Roadways, Environmental Science & Technology, 39, 826-836, https://doi.org/10.1021/es048715f, 2005.

Mahowald, N. M., Hamilton, D. S., Mackey, K. R. M., Moore, J. K., Baker, A. R., Scanza, R. A., and Zhang, Y.: Aerosol trace metal leaching and impacts on marine microorganisms, Nature Communications, 9, 2614, https://doi.org/10.1038/s41467-018-04970-7, 2018.

Mao, J., Fan, S., and Horowitz, L. W.: Soluble Fe in Aerosols Sustained by Gaseous HO2 Uptake, Environmental Science & Technology Letters, 4, 98-104, https://doi.org/10.1021/acs.estlett.7b00017, 2017.

Mao, J., Fan, S., Jacob, D. J., and Travis, K. R.: Radical loss in the atmosphere from Cu-Fe redox coupling in aerosols, Atmos. Chem. Phys., 13, 509-519, 10.5194/acp-13-509-2013, 2013.

Nriagu, J. O.: A global assessment of natural sources of atmospheric trace metals, Nature, 338, 47-49, https://doi.org/10.1038/338047a0, 1989.

Oakes, M., Ingall, E. D., Lai, B., Shafer, M. M., Hays, M. D., Liu, Z. G., Russell, A. G., and Weber, R. J.: Iron Solubility Related to Particle Sulfur Content in Source Emission and Ambient Fine Particles, Environmental Science & Technology, 46, 6637-6644, https://doi.org/10.1021/es300701c, 2012.

Paatero, P.: Least squares formulation of robust non-negative factor analysis, Chemometrics and Intelligent Laboratory Systems, 37, 23-35, https://doi.org/10.1016/S0169-7439(96)00044-5, 1997.

Paatero, P. and Tapper, U.: Positive matrix factorization: A non-negative factor model with

838 optimal utilization of error estimates of data values, Environmetrics, 5, 111-126,
839 https://doi.org/10.1002/env.3170050203, 1994.

840 Paris, R. and Desboeufs, K. V.: Effect of atmospheric organic complexation on iron-bearing
841 dust solubility, Atmospheric Chemistry and Physics, 13, 4895-4905,
842 https://doi.org/10.5194/acp-13-4895-2013, 2013.

843 Paris, R., Desboeufs, K. V., and Journet, E.: Variability of dust iron solubility in atmospheric
844 waters: Investigation of the role of oxalate organic complexation, Atmospheric Environment,
845 45, 6510-6517, https://doi.org/10.1016/j.atmosenv.2011.08.068, 2011.

846 Paytan, A., Mackey, K. R. M., Chen, Y., Lima, I. D., Doney, S. C., Mahowald, N., Labiosa, R.,
847 and Postf, A. F.: Toxicity of atmospheric aerosols on marine phytoplankton, Proceedings of the
848 National Academy of Sciences of the United States of America, 106, 4601-4605,
849 https://doi.org/10.1073/pnas.0811486106, 2009.

850 Phalen, R. F.: The particulate air pollution controversy, Nonlinearity Biol Toxicol Med, 2, 259-
851 292, https://doi.org/10.1080/15401420490900245, 2004.

852 Pye, H. O. T., Nenes, A., Alexander, B., Ault, A. P., Barth, M. C., Clegg, S. L., Collett Jr, J. L.,
853 Fahey, K. M., Hennigan, C. J., Herrmann, H., Kanakidou, M., Kelly, J. T., Ku, I. T., McNeill,
854 V. F., Riemer, N., Schaefer, T., Shi, G., Tilgner, A., Walker, J. T., Wang, T., Weber, R., Xing, J.,
855 Zaveri, R. A., and Zuend, A.: The acidity of atmospheric particles and clouds, Atmos. Chem.
856 Phys., 20, 4809-4888, https://doi.org/10.5194/acp-20-4809-2020, 2020.

857 Schroth, A. W., Crusius, J., Sholkovitz, E. R., and Bostick, B. C.: Iron solubility driven by
858 speciation in dust sources to the ocean, Nature Geoscience, 2, 337-340,
859 https://doi.org/10.1038/ngeo501, 2009.

860 Sedwick, P. N., Sholkovitz, E. R., and Church, T. M.: Impact of anthropogenic combustion
861 emissions on the fractional solubility of aerosol iron: Evidence from the Sargasso Sea,
862 Geochemistry, Geophysics, Geosystems, 8, https://doi.org/10.1029/2007GC001586, 2007.

863 Shelley, R. U., Landing, W. M., Ussher, S. J., Planquette, H., and Sarthou, G.: Regional trends
864 in the fractional solubility of Fe and other metals from North Atlantic aerosols (GEOTRACES
865 cruises GA01 and GA03) following a two-stage leach, Biogeosciences, 15, 2271-2288,
866 https://doi.org/10.5194/bg-15-2271-2018, 2018.

867 Shi, J., Guan, Y., Ito, A., Gao, H., Yao, X., Baker, A. R., and Zhang, D.: High Production of
868 Soluble Iron Promoted by Aerosol Acidification in Fog, Geophysical Research Letters, 47,
869 e2019GL086124, https://doi.org/10.1029/2019GL086124, 2020.

870 Sholkovitz, E. R., Sedwick, P. N., Church, T. M., Baker, A. R., and Powell, C. F.: Fractional
871 solubility of aerosol iron: Synthesis of a global-scale data set, Geochimica et Cosmochimica
872 Acta, 89, 173-189, https://doi.org/10.1016/j.gca.2012.04.022, 2012.

873 Slikboer, S., Grandy, L., Blair, S. L., Nizkorodov, S. A., Smith, R. W., and Al-Abadleh, H. A.:

874 Formation of Light Absorbing Soluble Secondary Organics and Insoluble Polymeric Particles
875 from the Dark Reaction of Catechol and Guaiacol with Fe(III), Environmental Science &
876 Technology, 49, 7793-7801, https://doi.org/10.1021/acs.est.5b01032, 2015.

877 Spokes, L. J., Jickells, T. D., and Lim, B.: Solubilisation of aerosol trace metals by cloud
878 processing: A laboratory study, Geochimica et Cosmochimica Acta, 58, 3281-3287,
879 https://doi.org/10.1016/0016-7037(94)90056-6, 1994.

880 Tao, Y. and Murphy, J. G.: The Mechanisms Responsible for the Interactions among Oxalate,
881 pH, and Fe Dissolution in PM2.5, ACS Earth and Space Chemistry, 3, 2259-2265,
882 https://doi.org/10.1021/acsearthspacechem.9b00172, 2019.

883 Wang, W., Liu, M., Wang, T., Song, Y., Zhou, L., Cao, J., Hu, J., Tang, G., Chen, Z., Li, Z., Xu,
884 Z., Peng, C., Lian, C., Chen, Y., Pan, Y., Zhang, Y., Sun, Y., Li, W., Zhu, T., Tian, H., and Ge,
885 M.: Sulfate formation is dominated by manganese-catalyzed oxidation of SO2 on aerosol
886 surfaces during haze events, Nature Communications, 12, https://doi.org/10.1038/s41467-021-
887 22091-6, 2021.

888 Wang, Z. Z., Fu, H. B., Zhang, L. W., Song, W. H., and Chen, J. M.: Ligand-Promoted
889 Photoreductive Dissolution of Goethite by Atmospheric Low-Molecular Dicarboxylates,
890 Journal of Physical Chemistry A, 121, 1648-1657, https://doi.org/10.1021/acs.jpca.6b09160,
891 2017.

892 Wong, J. P. S., Yang, Y., Fang, T., Mulholland, J. A., Russell, A. G., Ebelt, S., Nenes, A., and
893 Weber, R. J.: Fine Particle Iron in Soils and Road Dust Is Modulated by Coal-Fired Power Plant
894 Sulfur, Environmental Science & Technology, 54, 7088-7096,
895 https://doi.org/10.1021/acs.est.0c00483, 2020.

896 Ye, D., Klein, M., Mulholland, J. A., Russell, A. G., Weber, R., Edgerton, E. S., Chang, H. H.,
897 Sarnat, J. A., Tolbert, P. E., and Ebelt Sarnat, S.: Estimating Acute Cardiovascular Effects of
898 Ambient PM2.5 Metals, Environmental Health Perspectives, 126, 027007,
899 https://doi.org/10.1289/ehp2182, 2018.

900 Zhang, H., Li, R., Dong, S., Wang, F., Zhu, Y., Meng, H., Huang, C., Ren, Y., Wang, X., Hu,
901 X., Li, T., Peng, C., Zhang, G., Xue, L., Wang, X., and Tang, M.: Abundance and Fractional
902 Solubility of Aerosol Iron During Winter at a Coastal City in Northern China: Similarities and
903 Contrasts Between Fine and Coarse Particles, Journal of Geophysical Research: Atmospheres,
904 127, e2021JD036070, https://doi.org/10.1029/2021JD036070, 2022.

905 Zhao, Z., Luo, X. S., Jing, Y. S., Li, H. B., Pang, Y. T., Wu, L. C., Chen, Q., and Jin, L.: In vitro
906 assessments of bioaccessibility and bioavailability of PM2.5 trace metals in respiratory and
907 digestive systems and their oxidative potential, Journal of Hazardous Materials, 409,
908 https://doi.org/10.1016/j.jhazmat.2020.124638, 2021.

909 Zhong, L., Louie, P. K. K., Zheng, J., Yuan, Z., Yue, D., Ho, J. W. K., and Lau, A. K. H.:
910 Science–policy interplay: Air quality management in the Pearl River Delta region and Hong

Kong, Atmospheric Environment, 76, 3-10, https://doi.org/10.1016/j.atmosenv.2013.03.012, 2013.

Zhou, Y., Zhang, Y., Griffith, S. M., Wu, G., Li, L., Zhao, Y., Li, M., Zhou, Z., and Yu, J. Z.: Field Evidence of Fe-Mediated Photochemical Degradation of Oxalate and Subsequent Sulfate Formation Observed by Single Particle Mass Spectrometry, Environmental Science & Technology, 54, 6562-6574, https://doi.org/10.1021/acs.est.0c00443, 2020.

Zhu, X., Prospero, J. M., Savoie, D. L., Millero, F. J., Zika, R. G., and Saltzman, E. S.: Photoreduction of iron(III) in marine mineral aerosol solutions, Journal of Geophysical Research: Atmospheres, 98, 9039-9046, https://doi.org/10.1029/93JD00202, 1993.

Zhu, Y., Li, W., Lin, Q., Yuan, Q., Liu, L., Zhang, J., Zhang, Y., Shao, L., Niu, H., Yang, S., and Shi, Z.: Iron solubility in fine particles associated with secondary acidic aerosols in east China, Environmental Pollution, 264, 114769, https://doi.org/10.1016/j.envpol.2020.114769, 2020.